

MICROSCOPE Mission: on-orbit assessment of the Drag-Free and Attitude Control System

By Pascal PRIEUR,¹⁾²⁾ Thomas LIENART,¹⁾³⁾ Manuel RODRIGUES,⁴⁾ Pierre TOUBOUL,⁵⁾
Troelz DENVER,⁶⁾ John L. JØRGENSEN,⁶⁾ Anastassia M. BANG,⁶⁾ and Gilles METRIS⁷⁾

¹⁾Centre National d'Etudes Spatiales, 18 av Edouard Belin F31400 Toulouse, France

²⁾Department of Flight Dynamics

³⁾Department of Propulsion

⁴⁾ONERA, Département 'Physique, Instrumentation, Environnement, Espace', Chatillon, France

⁵⁾ONERA, Microscope space mission Prime Investigator, Palaiseau, France

⁶⁾Technical University of Denmark, Lyngby, Denmark

⁷⁾Université de la Cote d'Azur, Observatoire de la Côte d'Azur, CNRS, Géoazur, Valbonne, France

(Received June 21st, 2017)

Microscope successfully completed in November 2016 its on-orbit assessment. The paper begins with a brief description of the mission, the challenging performances the DFACS has to comply with and how they led to the hardware and software design. Then we go through the major phases of the commissioning months for DFACS, from the first switch-on of the scientific instrument, the star-trackers and the propulsion system until getting all of them in the same control loop and carrying out definitive tunings to reach full performance. At the end of the commissioning, we look over the most striking on-orbit observations: the linear and angular perturbations and the micro-perturbations. We finally point out the DFACS overall performances: the finest ever achieved on low earth orbit.

Key Words: Microscope, drag-free, accelerometers, cold-gas propulsion

Nomenclature (list of acronyms)

CGPS	Cold Gas Propulsion System
DF-TM	Drag-Free TM : mass (or combination of several masses) submitted to drag-free control
DFACS	Drag Free and Attitude Control System
DoF	Degree of Freedom
ECM	Electronic Control Module (propulsion)
EP	Equivalence Principle
Fep	Equivalence Principle observation Frequency
FFT	Fast Fourier Transform
Forb	Orbital Frequency
Fspin	Spin Frequency
GoG	Gradient of Gravity
MFS	Mass Flow Sensor (micro-thruster element)
mHz	milliHerz (10^{-3} Hz)
PRM	Pressure Regulation Module (propulsion)
STR	Star TRacker
TM	Test-Mass (we have 4 TM onboard, working by pair)
TSAGE	Twin Space Accelerometer for Gravity Experiment

1. Introduction

Microscope is a CNES-ESA-ONERA-OCA mission whose main objective is to progress in fundamental physics by testing the Equivalence Principle (EP) with an expected accuracy of 10^{-15} (see Ref. 1 for precisions about the mission and the satellite). The scientific instrument is a differential electrostatic accelerometer developed by ONERA. The more

than 300kg drag-free microsatellite was launched on April 25th 2016 into a 710km dawn-dusk sun-synchronous orbit for a 2-year mission.

The mission requires a drag-free satellite as well as a high accuracy attitude control. The Drag Free and Attitude Control System (DFACS) use the scientific instrument itself in the control loop for sensing linear and angular accelerations. A set of 8 cold gas proportional thrusters perform the 6-axis actuation. In mission mode, the propulsion subsystem continuously overcomes the non-gravitational forces and torques (air drag, solar pressure, etc.) in such a way that the satellite follows the test masses in their pure gravitational motion.

The paper is divided into three main sections:

- From a brief description of the Microscope mission, we will recall some of the most challenging performances and constraints that the DFACS has to comply with, and how they led to the hardware and software design
- Then, we draw a chronological overview of the commissioning months, highlighting the most interesting steps for the DFACS (see forthcoming Ref. 2 for the whole system point of view),
- We finally focus on the most striking on-orbit observations for DFACS: the linear and angular orbital perturbations, the micro-perturbations, the gas consumption, the overall 6 axis performances

2. From scientific objectives to DFAC design

2.1. Overview of the Microscope experiment

The MICROSCOPE mission, French acronym for MICRO Satellite with drag Control for the Observation of the Equivalence Principle, has been proposed in the early 2000s to continue and take advantage of the long experience of the ONERA's team in space accurate accelerometry and the team from Observatoire de la Cote d'Azur, OCA, in space geodesy and accurate trajectography. Furthermore, the Cnes MYRIADE family microsatellite line gave the opportunity of defining a challenging and ambitious mission, with the ESA cooperation for the procurement of the specific satellite propulsion system.

The primary scientific objective of the MICROSCOPE mission is the test of the universality of free-fall, which is one of the most well-known consequences of the Equivalence Principle (EP), with an accuracy of 10^{-15} .

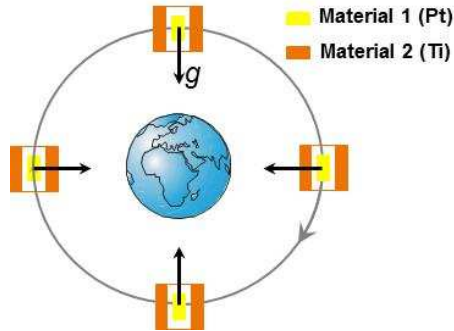


Fig. 1. Schematic view of 2 test-masses (TM), inertial mode

The in-orbit motion of two masses made of two different materials and falling in the Earth gravity field is controlled in an identical way, taking care that both masses are submitted exactly to the same gravitational field. The fine measurement of the monitored electrostatic potentials controlling the motion of the masses and breaking the experimentation symmetry provides the test signal.

$$\vec{s} = \vec{\gamma}_1 - \vec{\gamma}_2 = \delta \times \vec{g} \quad (1)$$

Where 'g' is the Earth gravitational acceleration ($\sim 7.8 \text{ m/s}^2$ at the flight altitude) and 'δ' is the equivalence principle violation parameter:

$$\delta = \left(\frac{m_{1g}}{m_{1i}} - \frac{m_{2g}}{m_{2i}} \right) \quad (2)$$

This experiment is referred as Weak Equivalence Principle (WEP) test. Until Microscope, the best estimate of the Eötvös parameter 'δ' was null (no violation) with an uncertainty of about $\pm 1.8 \times 10^{-13}$.

The scientific instrument TSAGE is actually composed of two 'differential' accelerometers, each including two cylindrical and concentric test masses. The masses are made of the same material for the first one (called SU-REF) which is dedicated

to assess the accuracy of experimentation and the mass materials are different for the second one (called SU-EP).

2.2. The orbit, attitude guidance and frequency 'Fep'

A dawn-dusk sun synchronous orbit (altitude $\sim 710 \text{ Km}$, RAAN $\sim 18 \text{ h}$) was chosen for Microscope. This orbit is fully sunlit, except during 3 months around the summer equinox (from May 9th to August 4th) where eclipses occur around the southern pole (see Fig. 2).

Inertial sessions:

The satellite is inertially pointed (i.e. it just follows the one degree per day drift of the orbital plane). The main axis of the accelerometer ($X_{inst} \sim Z_{sat}$) remains in the orbital plane. According to Eq. (1), the EP hypothetical violation signal is modulated at the rotational frequency of the 'g' in satellite frame (Fep):

$$F_{ep(inertial)} = F_{orb} \approx 0.17 \text{ mHz} \quad (3)$$

Rotating sessions:

The satellite is set in rotation around the orbit normal ($Y_{inst} \sim X_{sat}$) at the frequency F_{spin} in order to increase the rotational frequency of the 'g' in satellite frame:

$$F_{ep(rotating)} = F_{orb} + F_{spin} \quad (4)$$

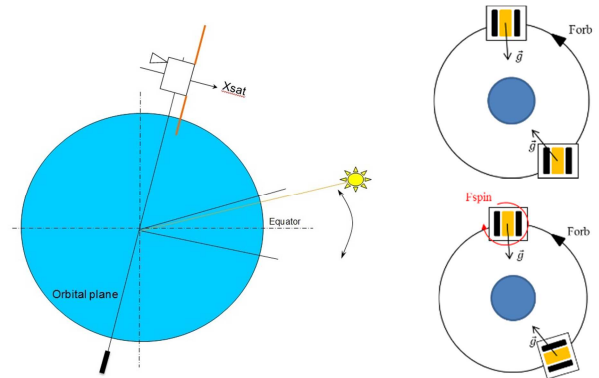


Fig. 2. The orbit (left) and the attitude guidance: inertial (top right) and rotating (bottom right)

The rate of spin is a design driver for DFACS, the satellite was qualified and launched with two values only: $F_{spin1} = 3.5$ rotation per orbit and $F_{spin2} = 4.5$ rotation per orbit. The resulting Fep frequencies are respectively $F_{eps1} \sim 0.76 \text{ mHz}$ and $F_{eps2} \sim 0.93 \text{ mHz}$.

The sessions were designed to last 8 days (120 orbits) in inertial mode and 1.5 days (20 orbits) in rotating mode. The session's length T is a high level system parameter which determines the reduction (factor \sqrt{T}) of stochastic terms while harmonic ones remain incompressible.

In addition, a panel of specific sessions is dedicated to the accelerometer calibration. All of them are based on an inertial pointing, some consist in adding harmonic signal to the DF-TM output (linear stimulation), others require angular oscillations of 0.05 rad (2.9 deg) at $F_{cal} \sim 1.3 \text{ mHz}$. These sessions are shorter (5 or 10 orbits).

2.3. Drag-free requirements: motivation and challenges

The Eq. (1) involves a difference between two measurements which have their own scale factor imperfection K_1 and K_2 . The real signal S' then depends on the 'differential mode' acceleration (the original unknown S signal) but also on the 'common mode' acceleration.

$$\begin{array}{c} \left[\begin{array}{c} \gamma_1 \\ \gamma_2 \end{array} \right] \\ K_1 \neq K_2 \end{array} \quad \bar{S}' = (1+K_1)\bar{\gamma}_1 - (1+K_2)\bar{\gamma}_2 \\ = \underbrace{(\bar{\gamma}_1 - \bar{\gamma}_2)}_{\text{diff mode}} + \underbrace{\left(\frac{K_1+K_2}{2}\right)(\bar{\gamma}_1 + \bar{\gamma}_2)}_{\text{diff mode}} + \underbrace{(K_1-K_2)\left(\frac{\bar{\gamma}_1 - \bar{\gamma}_2}{2}\right)}_{\text{common mode acceleration}} \quad (5)$$

The differential scale factor (K_1-K_2) matching accuracy is limited to 0.015% ($1.5e-4$). To achieve the overall mission objective ($1e-15$ on δ , that is $7.8e-15m/s^2$) for every session of measurement, with a large number of contributors to the performance, it was decided to limit this term to one part out of 40, i.e. $2e-16m/s^2$. Hence, the common mode acceleration (drag-free performance) must remain under $1e-12 m/s^2$ at the frequency of scientific interest F_{ep} .

While some phenomena are harmonic (Tone Error) and others stochastic (Random Error), they were quoted separately considering the factor $\sqrt{T}=300$, corresponding to a 20 orbit session.

What does 'drag-free' mean?

JW Conklin,¹⁰ explains quite well what a drag-free satellite is. He distinguishes the 'traditional' definition of drag-free where the test mass is freely floating and the 'accelerometer mode' drag-free where the mass is suspended and the satellite provides an additional layer of control. The last definition is applicable to Microscope, that's why the acronym AACS (Attitude & Accelerations Control System) is generally preferred to DFACS.

This observation is of first interest to understand our management of TSAGE linear biases: we are allowed to subtract the 'estimated linear biases' from the measurement of the DF-TM. Moreover, with 'traditional' drag-free the angular motion of the TM remains a limit (the satellite cannot easily follow), on Microscope the long term attitude control of the satellite is based on the star-tracker measurement and not on the TM angular outputs.

Once the DFACS active, a frequency based separation operates: the s/c propulsion system compensates for external perturbations (6 DoF) at low frequency (until some tens of mHz) while the suspension of the TM (6 DoF) is loaded by biases and higher frequencies (transient and spikes).

Attempts to fly Microscope in 'traditional' drag-free mode could be tested at the end of the mission, for a limited period of time. TSAGE delivers the positions as well as the accelerations of the masses: the DFACS could use it to drive the propulsion.

Where is the challenge?

Without drag-free control, the performance @ F_{ep} is about $1e-8m/s^2$. A minimal rejection 90dB is then required to reach $1e-12m/s^2$. The challenge becomes to drop the gain above F_{ep}

(see §2.5) quickly enough to keep stability margins. Spikes are also a challenge as far as their 'Dirac shape' raise up the entire spectrum.

2.4. Attitude requirements: motivation and challenges

The Eq. (1) can also be adapted to take into account the miscentring of the 2 test-masses which is limited by technology to about $20\mu m$. This distance induces 'inertial' and 'GoG' terms.

$$\begin{array}{c} \left[\begin{array}{c} \gamma_1 \\ \gamma_2 \end{array} \right] \\ O_1 \neq O_2 \end{array} \quad \bar{S}' = (\bar{\gamma}_1 - \bar{\gamma}_2) + \bar{\Omega} \wedge (\bar{\Omega} \wedge \bar{\Delta}) + \dot{\bar{\Omega}} \wedge \bar{\Delta} \\ \bar{\Delta} = O_1 \bar{O}_2 \quad (6)$$

The 'inertial' ones depend on the attitude control. With an upper bound of $2e-16m/s^2$ for each term, it comes:

- $\dot{\bar{\Omega}}@F_{ep}$ is limited to $1e-11 rad/s^2$ in inertial and rotating modes
- $\bar{\Omega}@F_{ep}$ is limited to $1e-9 rad/s$ in rotating mode

Where is the challenge?

It is worth to notice that $1e-9rad/s @F_{eps}$ (about $1mHz$) corresponds to an attitude stability of $0.16\mu rad @F_{eps}$. This performance is clearly out of feasibility for a star tracker.^{3,4} The challenge is the attitude estimation.

DFACS performances

Actually, the scientific mission analysis addresses some combinations between harmonic signals $k.F_{ep}$ (involving for example the eccentricity of the orbit) which give F_{ep} signal. Requirements at many frequencies (F_{ep} , $2F_{ep}$, $3F_{ep}$) are mandatory. Moreover, non-linearities in the extraction of δ are taken into account through rejection templates. Ultimately, the rules for quantifying the DFACS performances are complex.⁵

2.5. The DFACS final design: hardware and software

The DFACS is designed to achieve the drag-free as well as the attitude control performance, basically $1.10^{-12} m/s^2$ and $1.10^{-9} rd/s$ in the bandwidth of scientific interest (F_{ep}).

To meet these stringent requirements, the DFACS relies on the payload accurate accelerations measurements for both linear and angular control.

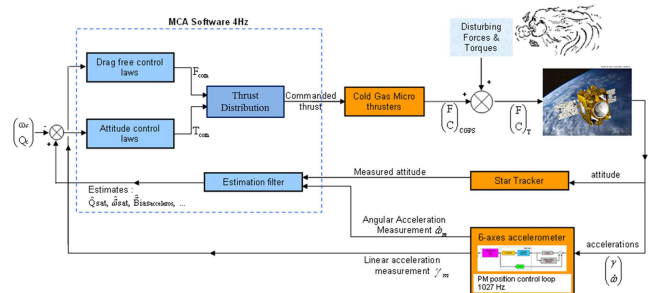


Fig. 3. DFACS control loop

Linear accelerations are directly used by the drag free control whereas the attitude estimation is the result of hybridization

between STR measurements and angular accelerations.³⁾ Then a set of 8 cold gas GAIA-like thrusters allow to accurately perform the commanded force and torque. The DFACS control loop is illustrated in Fig. 3. As much as 38 loops are closely involved: 6 times 4 loops for the suspension of the test masses, 6 loops for DFACS itself and 8 loops for the regulation of the thrusters. We call DF-TM the mass (or the combination of masses) used as source for the drag-free (system parameter of every session).

Hardware

The scientific instrument TSAGE is set at the center of the platform in order to minimize the gravity gradient (GoG) between the satellite center of mass G and the TM location (usually called A). As we have 2 instruments (EP and REF) distant of 171mm, G was set approximately at the center of A_{EP} and A_{REF} . The $A_{EP}A_{REF}$ direction is also aligned with X_{sat} , and X_{sat} is close to an inertia eigenvector. All is designed to minimize inertial effects (centrifugal force and gyroscopic torques) in rotating mode.

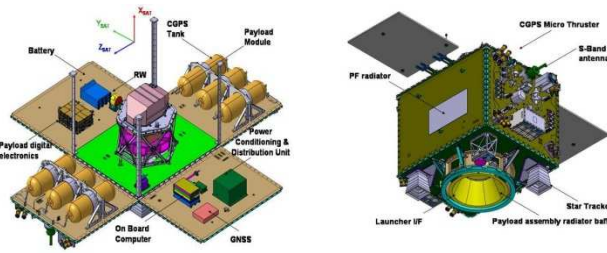


Fig. 4. Satellite layout and DFACS hardware

The propulsion configuration: 8 thrusters (+1/1 redundancy) located on the corners of 2 identical panels (Z_p and Z_m) was optimized through a comparison between the 6 DoF ‘control authority domain’ and the 6 DoF ‘perturbations domain’. We quickly observed that torques were higher than forces and were quite symmetrical. That’s why the nominal thrusters are located on the corners with maximum torque efficiency. The star tracker is inherited from Myriade line of platforms.¹¹⁾ Some intensive in-flight tests were performed on Picard and Prisma,⁶⁾ to assess the low frequency performances. The geometrical configuration (2 optical heads co-aligned but twisted) results from the orbit and attitude geometry: ‘ $-X_{sat}$ ’ is the only direction compatible with the earth exclusion angle. We wanted neither commutation between heads (2Fep frequency) nor albedo flux entry (Fep). We accept lower performance about line of sight (X_{sat}).

Figure 4 shows the satellite: 301.4Kg at the beginning of life (included 2x8.35Kg of Nitrogen), 125watts, 1380x1040x1580cm size.

Software

Figure 5 presents the software architecture of the DFACS. The ‘MSP’ mode on top of the figure performs a fine attitude

control thanks to the STR measurement and CGPS torques. This mode is also used in case of collision avoidance procedure but its main function is to be the gate for the drag-free mode ‘MCA’ in which one or several TM of TSAGE are used. The MCA mode is made of many tunings: the MCA3 (attitude only) and MCA6 (6 axis control) have low gain robust control, used to estimate the angular bias of the DF-TM, to change the attitude guidance, etc. The MCAcp performs an automatic sequence of test for the thrusters (see §3.4). The other high gain tunings are dedicated to inertial sessions (MCAi), rotating session velocity 1 (MCAs1), etc.

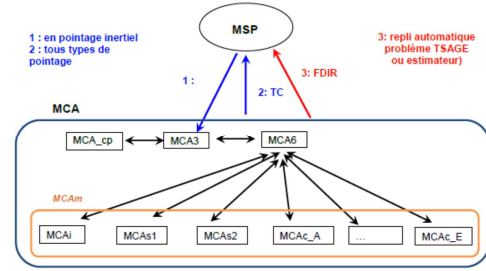


Fig. 5. DFACS software architecture

We enter in a mission mode with a simple telecommand; several attitude controllers are successively used until the nominal one. The attitude control has so huge gains that they are not activable directly.

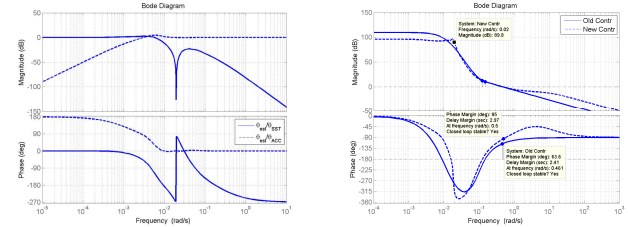


Fig. 6. Specific hybridization (left) and drag-free controller (right) in Rotating mode (new control: adapted to SpinMax)

The biggest challenges for DFACS consist in estimating the attitude in rotating mode and keeping positive margins to the control loops: as we said above, the DFACS loop is set between the DF-TM suspension control loops and the thrusters control loop. We managed to have a net delay margin about 1 second @0.075Hz.

3. On-orbit assessment

3.1. Overview of the commissioning months

This victorious campaign is related from DFACS point of view, see forthcoming Ref. 2 for a general view of the whole battlefield.

The Microscope spacecraft was launched from Kourou on 25 April 2016 (Soyuz VS14). The orbit injection was nearly perfect; the AOCS acquisition mode did the job as foreseen: it quickly damped the angular rate, sped-up the kinetic wheel

and drove the satellite X axis toward the sun. After usual verification, we uploaded the navigation and attitude guidance plans and switch to ‘MGT’ mode. This coarse transition mode, based on magnetic measurement and actuation, will then control the satellite. It was time to power-on TSAGE, to verify the gold wires and to unfold the test masses. This step was completed on time; the levitation of the test masses (full range mode FRM) was a success. Meanwhile, the propulsion subsystem went through its commissioning steps: opening the high pressure valves, reducing the plenums to operational pressure, performing the first calibration of the MFS, testing the 8 nominal thrusters.

The first surprise came from the star tracker: plenty of ‘big bright object’ (BBO) status were reported in the telemetry over the northern part of the orbit, associated with invalid quaternions.

On May 11th the satellite was controlled for the first time in mode MSP: attitude control with STR measurements and CGPS actuation. The qualification of the collision avoidance procedure was successfully tested on May 12th.

On 2016 June 07th, the satellite was controlled for the first time in drag-free mode MCA. On June 17th, during an inertial scientific session, a sudden demotion to MSP was automatically triggered on-board. The experts later determined that the SU-REF front end electronics suffers from partial failure. Since that time, the SU-EP and the SU-REF are operated separately. After the eclipse season, the scientific team decided to give up inertial sessions and to increase Fep: the SpinMax sessions were created. We decided to replace the previous Fspin1 tunings by the SpinMax ones, Fspin2 remains unchanged. The Table 1 shows that the rotation rate is sharply increased to 17.5 rotations per orbit, Fep reaches 3.11 mHz.

Vitesse	rad/s	Hz	RpO(**)	période(sec)
Worbital W0	1.056703E-03	1.681796E-04	1.00	5946
Wspin1	1.849231E-02	2.943142E-03	17.50	340
Weps1	1.954901E-02	3.111322E-03	18.50	321
Wspin2	4.755165E-03	7.568080E-04	4.50	1321
Weps2	5.811868E-03	9.249876E-04	5.50	1081

Table 1 : the couple (Fspin, Fep) after creation of the SpinMax

On November 2016, the commissioning phase was over.

3.2. The scientific instrument TSAGE

The assessment of TSAGE is a too big story; it will be related in Ref. 2.

3.3. The star tracker

The long term attitude recovery is provided by the *Micro Advanced Stellar Compass* (μ ASC); an autonomous, non-magnetic, 3-axes star tracker that provides arc-second attitude recovery.¹³⁾ It is designed and fabricated at the *Technical University of Denmark* (DTU) and has extensive flight heritage from scores of satellite missions. *The Data Processing Unit* (DPU) supports up to four *Camera Head Units* (CHUs), enabling both redundancy and operational

constraint reduction.¹⁴⁾ The extreme attitude knowledge requirement from Microscope is ensured by the heritage μ ASC augmented with a few optimizations:

- *Dual head configuration*: Microscope features two CHUs heads biased 90deg around boresight. This configuration will ensure attitude information optimally, making best use of the rectangular field of view of the instrument.
- *Thermal gradient free design*: A novel thermal design ensures a gradient-free thermal coupling. Thermal radiation is effectively blocked between the inner and outer baffle stage and conduction between I/F plate and CHU is arranged such that a changing I/F plate temperature will lead to mechanical translation only.
- *Roll accuracy performance optimization*: Star trackers feature anisotropic noise characterization, providing an order of magnitude better pointing accuracy (along boresight) than roll accuracy (about boresight). Since the roll performance is of key importance to Microscope, the star tracker has sacrificed part of the pointing accuracy to provide better roll performance. These algorithms were tested successfully on PICARD prior to Microscope to demonstrate the concept.

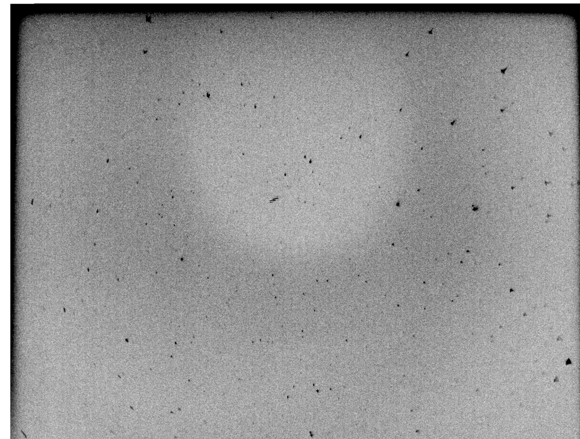


Fig. 7. Inverted image from CHU-2 showing the stray light (in black) at top, right and left edges

Since the first orbit after power-on, stray light manifestations were observed on both CHUs. Over the northern part of the orbit, the impingement was so manifest that it prevented successful attitude determination. The baffles had been optimized to discard from earth and moon stray-light; hence their geometry was different from classical two-stage Myriade ones. Something had gone wrong somewhere in the process of integration. An example image of the stray light (inverted) is shown in Fig. 7 and shows a heavy manifestation in the top, left and right image borders.

A working group dedicated to the mitigation was setup between CNES and DTU. Massive images from both CHUs were downloaded to fully characterize the effect, and how it evolved over the orbit. Based on the rich imagery, an ‘‘edge

clipper” augmentation of the flight software was developed that can ignore the stray light impinged part of the source images. This SW was uploaded on June 1st. It is still active, efficient and stable through the seasons. It has no measurable impact on performance. The problem was smartly fixed while the commissioning was going-on for the rest of the satellite to reduce commissioning delays.

3.4. The cold gas propulsion system

Each one of the 8 proportional thrusters has to comply with the operational range (1 μN to 300 μN), the response time (<250 ms @63%) and a thrust noise (<1 $\mu\text{N}/\sqrt{\text{Hz}}$, between 0.1 and 10 Hz). The CGPS architecture is exposed in Ref. 8; the MTs are manufactured by the Italian firm Leonardo Spa. They have been qualified within the frame of the Esa GAIA program and are used on Lisa pathfinder and Euclid Esa’s missions.⁹⁾

The working principles as well as the thruster’s design are exactly the same as on the GAIA spacecraft. However, CNES’ requirements in terms of control loop performances (time response) are more stringent than on GAIA. The electronic control module (ECM) is also tailored-made for Microscope, as the system architecture is specific.

MFS zeroing

The thruster’s performance is based on a closed loop control (see Ref. 9): the micro thrust regulation is realized by operating the Thruster Valve (TV) in closed loop control with a Mass Flow Sensor (MFS) positioned upstream the TV and acting as the feedback sensor of the thrust closed loop control. The measured flow (related through the specific impulse to the thrust level) is used to control the degree of opening of the thruster valve in order to “chase” the commanded micro thrust “set point”.

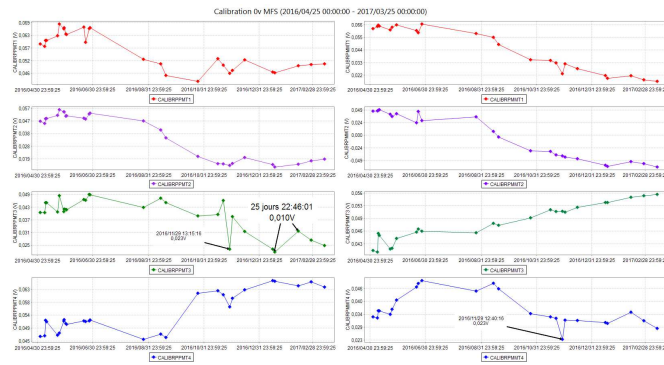


Fig. 8. Observed MFS biases (‘zeroing’ procedure) over 11 months

The stability over time of the MFS biases (voltage for null flux) determines the effective idle set point, fixed to 2.5 μN for Microscope. The biases are periodically calibrated thanks to a specific operational procedure (Zeroing). Figure 8 shows the evolution of the estimated biases for 11 months: if we except specific cases (zeroing performed on instable conditions), the evolution of the biases are lower than 10mV over a month, i.e. 1.4 μN . Actually, with a 2.5 μN idle set point, we do not

observe any problem of control: no lift-off delay or control oscillation.

Thrust calibration via TSAGE

The MCAcp mode stabilizes the s/c in inertial attitude and then activates the thrusters one by one for 10 seconds. Figure 9 clearly demonstrates the efficiency of the CGPS and the sensitivity of TSAGE. On top appear the commands: each one of the 8 thrusters is successively commanded to 5 μN while the others remain to idle (2.5 μN). The accelerations of the s/c seen by the 4 TMs are displayed below (example of Y axis). One can see the rise and fall time; such an acceleration step (2.5 $\mu\text{N}/301.4\text{Kg}=8.3\text{e-}9\text{m/s}^2$) is easily measured here with a good signal to noise ratio.

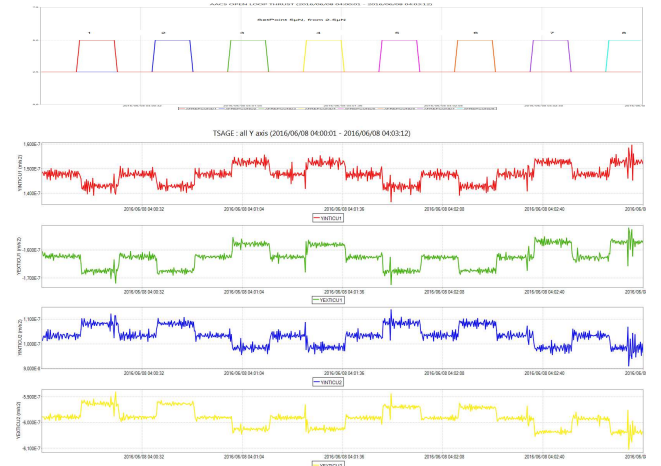


Fig. 9. DFACS OPEN LOOP THRUST (setpoint 5 μN , from 2.5 μN)

Figure 10 highlights with an example the dynamics of both CGPS and TSAGE. The blue line displays the set point of a thruster (4Hz telemetry from ECM) and the red line (4Hz telemetry from TSAGE) is the resulting acceleration measured by the external mass of EP (the titanium TM) about Y axis.

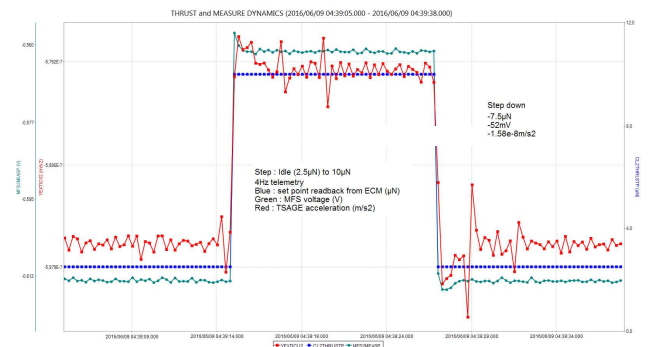


Fig. 10. A step 2.5 to 10 μN , thruster setpoint and TSAGE measure

Even if some fine correction of synchronization should be made (the read-back from ECM has a 250ms delay while TSAGE measure is advanced of a fraction of 250ms), one can observe the rise and fall time: the response time of the chain (thruster+TM suspension) is consistent with predictions

(250ms@63% for the thruster and 1.8Hz low pass filter for TSAGE). The green line (MFS voltage) confirms the amazing precision of the thruster's control loop. For memory, such a step means a $7.5\mu\text{N}/(g_0 \cdot \text{ISP}) \sim 15.3$ micrograms per second of gas flux ! In addition to dynamics of both CGPS and TSAGE, the precision of the whole system is remarkable (rise/fall symmetry, etc.).

Figure 11 displays the 6 axis measurement of one TM (4Hz telemetry) when a step from idle ($2.5\mu\text{N}$) to $100\mu\text{N}$ is successively commanded to each one of the 8 thrusters. The linear acceleration lies on the right side of the graph while the left side presents the angular accelerations. Both thrust control loop and mass suspension loop have a slight overshoot, no surprise to find quite large overshoots on such an experiment. It is worth to notice the excellent behavior of TSAGE on angular axes.

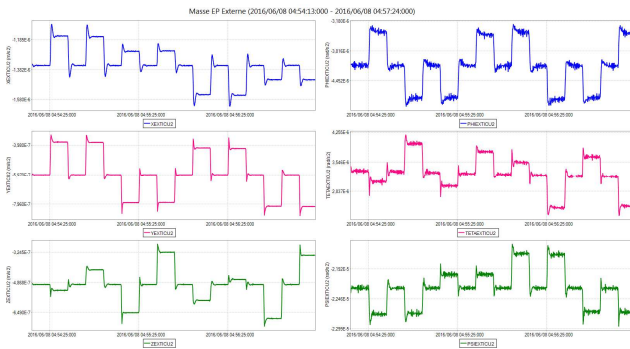


Fig. 11. AACS OPEN LOOP THRUST, setpoint 100microN, 6 axis measure EPext (titanium TM)

As we have 4 TM, each one delivering signals like Fig. 11, and we accurately know the locations and orientations of both the TM and the thrusters, we tried to estimate the 'real' 6 axes acceleration of the s/c. Our first idea was to consider TSAGE as a perfect accelerometer and to observe the real thrust. We failed to find consistent estimates. Actually we have significant cross axis coupling in TSAGE (except toward the most sensitive axis), specifically from linear to angular. Symmetrically, the observation the TM sensitivity 6x6 matrix considering the real acceleration as an input (given model of propulsion) was also a dead-end. The experiment involves too much parameters playing together: it's useful to confirm a model but not to identify without ambiguity.

Anomalies

The piezo-disks driving the thruster's valve have a highly hysteretic behavior; some oscillations of the improved control loop had been observed on ground tests, imputed to the 2 bar absolute inlet pressure. No such problem was observed in flight with an inlet pressure of 1 bar, the behavior of the control loop is quite perfect. Our interpretation is that as the flow is sonic the inlet pressure acts as physical gain on the 'plant' and the control loop has limited stability margins: less

than 6dB (ratio 2) at some thrust level.

Nonetheless, an unexpected functional issue happened. Indeed, several losses of communication between the on-board computer and one of the 2 ECM have occurred over the first weeks of operation. This issue is still under investigation, it has been by-passed thanks to a thermal control adaptation. Indeed, it seems that some electronic components are thermally sensitive.

3.5. The test of collision avoidance manoeuvre

A test of collision avoidance manoeuvre was performed on 2016 May 12th. In MSP mode (see §2.5), the resulting propulsion force is nominally commanded to null. For 56 minutes, we commanded a $-360\mu\text{N}$ force about X local orbital. The semi-major axis was reduced of 6.74m (+/- 1 cm) according to the fine orbit restitution.¹²⁾ The observed efficiency of the manoeuvre was -11.2%.

This observation is consistent with many others: the CGPS is under-calibrated: under-efficient and under gas consuming in the same ratio. The interpretation of this characteristic (it is not a problem as far as all the thrusters are equally affected) remains to do.

3.6. First steps into drag-free modes

All types of attitude guidance,⁷⁾ were tested in MSP mode: inertial, rotation, sinus, etc. We could estimate the acceleration biases (6 axes for each one of the 4 TM). As mentioned in §2.3, the drag-free control leaves the static load to the TM suspension: we do not search to discriminate between TM linear biases and static environmental perturbation (such as constant solar pressure or GoG). The best estimates of biases are uploaded in order to be removed from to TSAGE measurements as soon as they come into the DFACS preprocessing.

On June 7th we could come in MCA3 in inertial attitude: we observed the expected convergence of the attitude estimation, the right behavior of TSAGE as angular accelerometer. Moreover, we feared 'CPU overload' on the central OBC which has to handle many equipment and perform heavy calculations in DFACS SW. All went perfectly.

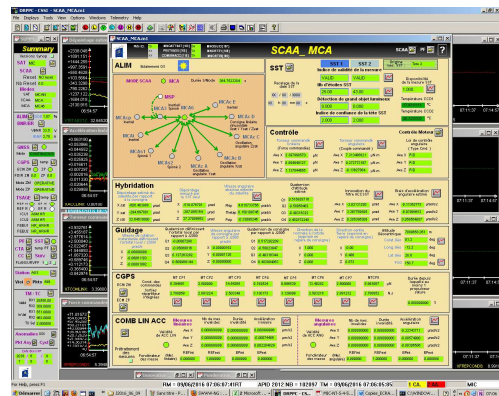


Fig. 12. 2016 June 9th, first experience of CNES in drag-free mode (real time display)

On June 9th (Fig. 12) we could enter in MCA6 and obtain the first drag-free experience in the history of CNES. The DF-TM was set on the external REF (the ‘big’ platinum TM). The 38 control loops (see §2.5) were working properly together. We observed low thrust commands: the biases management was correct, the satellite perturbations was within the predictions (magnetic torques, air drag, etc.), and the CGPS was 6 axis efficient.

4. DFACS performances

4.1. General behavior

Once the MCA6 assessed, we could tight the loops: enter into the mission modes which have huge control gains as well for drag-free as for attitude control. It was made first for inertial session MCAi, all went has expected. After the summer break (eclipses and electrical issues investigations) we could test the rotation mode MCAs (2016, September 1st). The original hybridization filter,³⁾ behave has expected.

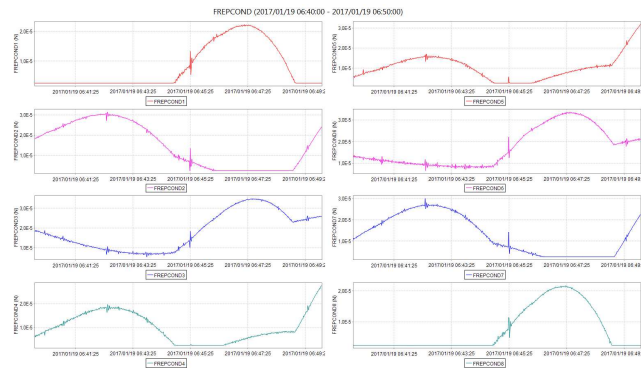


Fig. 13. Thrust set points for 10 minutes (Rotating MCAs2)

Figure 13 shows the telemetry (4Hz) of the thruster’s set points (panel Zp on the left and Zm on the right) over 10 minutes in rotating mode MCAs2. We first observe the low load of the thrusters (the Y scale is 0 to 40 µN only) and their general shape: periods at idle (2.5µN) followed by a very clean lift off (sudden change of slope without any oscillation), smooth domes and clean landing back to idle. Even with huge control gains (see Fig. 6), it is also remarkable to obtain so low noise on the propulsion commands. This observation justifies a design driver for the control loop of the thrusters: we look for fast response time but for very small steps (+/-2µN). From time to time, a spike appears on the DF-TM and induces a response on the propulsion.

4.2. The orbital perturbations

In matter of perturbations, there are clearly two worlds: one (inertial and slow rotating mode) is dominated by magnetic torques and the second (SpinMax rotating mode and sinus attitude profiles for instrument calibration) is respectively dominated by gyroscopic torques and by guidance torques. Both are dominated by torques, the drag-free control requires very low thrust.

The following Table 2 presents the main harmonic components of the DFACS control force and torque (F,C) for a slow spin session.

Forces

The air drag acts mainly on the orbital plane (YZsat) and at Fep: it is measured around 3µN only (for a cross section of $S_Y \sim 1.52m^2$ and $S_Z \sim 1.12 m^2$). The solar pressure, constant about Xsat, was observed during the eclipses season: 12µN for $S_X \sim 1.96m^2$. When the sun is distant from the orbit normal, the solar pressure produces a force about Y and Z axis at Fspin frequency, visible here around 1µN. The 1.52µN (Y, 2Fep) is not only explained by the GoG between the DF-TM and the satellite CoG (evaluated to 0.4mm along each axis of the orbital plane) but probably mostly results of a ‘torque to force’ coupling on the CGPS: a coupling of 3% from $C_x = 42.5\mu N.m$ to Fy. The drag-free control loop then see the coupling as a perturbation.

Torques

The torques are dominated by magnetic and gravity gradient (2Fep). The Fspin harmonic is also from secondary magnetic origin. The gyroscopic torques (static, Y and Z axis) caused by non-diagonal inertia terms stay low at this spin rate (4755µrad/s).

MCAs2 - SESSION 86 EPR_V2DFIS1_01_SUEP 28/09/2016 01:04:33 au 06/10/2016 07:16:36								
Force (µN, Rsat)	X	Y	Z	Torque (µN.m, Rsat)	X	Y	Z	
Average	0.21	3.19	19.54	Average	-0.96	7.66	12.06	
st.dev Sigma	0.47	2.48	1.92	St.dev Sigma	33.85	9.21	5.41	
forb	0.23	0.02	0.02	forb	0.20	0.03	0.02	
fspin	0.03	1.31	1.23	fspin	0.92	3.48	2.66	
1*fep	0.03	2.71	2.28	1*fep	0.09	0.39	0.12	
2*fep	0.17	1.52	0.29	2*fep	42.50	1.37	0.98	
3*fep	0.01	0.05	0.07	3*fep	0.03	0.01	0.02	

Table 2 : commanded force and torque for a slow rotating session MCAs2

When we decided to increase the spin rate (SpinMax sessions), we had to remember that the inertial accelerations are ω_{spin}^2 dependent: the gyroscopic torques become preminent ~92µN.m and 185µN.m about Y and Z axis

$$\vec{C}_{GR} = \omega_{spin}^2 \begin{pmatrix} 0 \\ -Ixz \\ Ixy \end{pmatrix} \quad \text{with} \quad \begin{matrix} I_{sat} = [58.5 \ 0.54 \ -0.27; \ 0.54 \ 60.9 \ 0; \ -0.27 \ 0 \ 47.5] \text{ Kg.m}^2 \\ W_{spinmax} = -18492e-6 \text{ rad/s;} \end{matrix}$$

The centrifugal force (acting as a linear bias in the orbital plane) was serendipitously low, thanks to a satellite centering much better than required (<0.4mm).

4.3. The micro-perturbations (‘clanks’)

Microscope was designed to avoid ‘clanks’, strict rules were respected and many tests were performed to this aim. Spikes measured over $3e-8m/s^2$ had to remain exceptions. Considering a 2Hz frequency bandwidth of TSAGE and a 200Kg satellite (old hypothesis), this spikes basically corresponds to a sudden movement of 36µm x gram.

An exhaustive classification of spikes observed in flight is still going on. If we exclude the season with eclipses, we

observe that the density of spikes is very dependent on the distance between the sun and the orbit normal (Xsat).

A very specific signature referred as ‘the three spike brothers’ is often observed (see Fig. 14): three spikes distant of 30 to 45 seconds from each other periodically appear about Zinst (i.e. Ysat) axis. The period depends on the attitude guidance, apparently a combination between the orbital position and the sun direction. Fortunately, their projection on Xinst (science axis) is very low. The origin could be a thermo-mechanical hysteretic cycling of the solar array folding mechanism illuminated by the solar flux (three parts located on every Y panel).

When the sun is close to the orbit normal (e.g. session 218, 120 orbits at the beginning of March), almost no clanks is visible. On the other hand, we observe a very little number of larger spikes probably caused by hyper velocity impacts (HVI). We do not observe spikes coming from propulsion panels (fluidic circuitry and mechanic PRM).

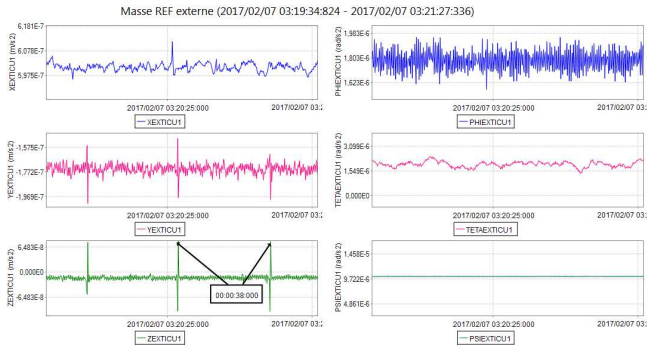


Fig. 14. The ‘three spike brothers’ (inertial guidance)

4.4. Gas consumption

The following Fig. 15 belongs to first operational importance. The gas consumption is accounted in gram per orbit per panel for every type of session.

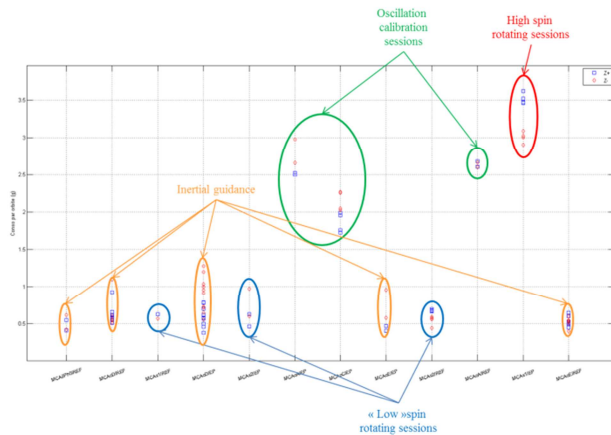


Fig. 15. Statistics of gas consumption

Obviously, gas consumption is directly linked to external perturbations (§4.2) and few attitude guidance require

accelerations. It is remarkable to notice that the mass of the satellite has no impact on the gas consumption while its inertia plays a second role through the gravity gradient torque and the starring role in SpinMax (through the non-diagonal terms). A good management of linear biases (see §3.6.) enables a minimal and symmetrical consumption between the two panels.

The gas consumption observed in flight looks like the best cases foreseen on the Monte-Carlo simulations. An inertial or slow rotation session uses 0.5 grams per orbit per panel (average thrust of about 20μN per thruster), but a SpinMax session swallows 3 to 3.5 grams/orbit/panel. While idle remains set to 2.5μN, the thrusters were allowed to throttle until 500μN in order to overcome the transients to commute to SpinMax sessions. The steady state load reaches 200μN on two thrusters, staying into the performance domain.

Return of experience

If we had anticipated the SpinMax mode (>1deg/s spin rate), we would have installed mass trim mechanisms (movable masses) in order to equilibrate the satellite spin axis and save gas (as GPB did, see Ref. 10).

4.5. Drag-free performances

The drag-free performance is measured through the DF-TM linear output. We typically observe a residual acceleration comparable to Fig. 16: the performance @Fep is done by air drag (3μN) braking the 300Kg satellite with a 90dB drag-free rejection. The control gain quickly drops above Fep(SpinMax), that is 3.11mHz. The first bump comes from a transmission of STR stochastic noise, as the second one is intrinsically due to the TM suspension. Isolated spectral lines are observed around 1Hz and 2Hz, caused by aliasing at the time of down sampling 4Hz. This marginal phenomenon is reduced since the upload of a new TM suspension control (Feb 2017).

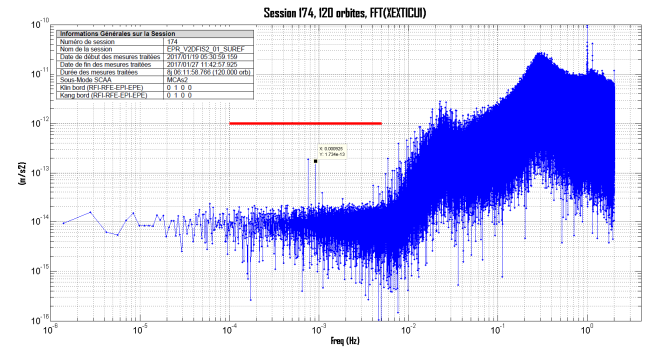


Fig. 16. FFT of the residual linear acceleration (slow rotating mode, 120 orbits)

The following Table 3 presents the evaluated performance of the same session (#174). The drag-free performance (top left bloc) about Xinst~Zsat is 1.74e-13m/s² @Fep (~0.925mHz). The performance is even better about Xsat (orbit normal)

which is faintly perturbed. One can observe the attitude control performance, specifically the angular rate stability @Fep which was a design driver (1e-9rad/s) in such rotating session: we demonstrate a performance of 3.79e-10rad/s @fep. As said before, the rules for quantifying the DFACS performances are complex,⁵⁾ but the observability of the real performance is quite good thanks to the redundancy of sources (4 TM x 6 DoF and 2 star tracker optical heads).

Fep (mHz) 0.92499319			
Bilans Session 174			
	Xsat	Ysat	Zat
Residual linear acceleration (m/s²)			
DC	5.20E-14	5.99E-14	2.20E-13
@fep	1.35E-14	2.05E-13	1.74E-13
@2fep	9.11E-14	1.54E-13	5.05E-15
@3fep	2.25E-14	1.99E-13	1.74E-13
Attitude error (rad)			
DC	8.28E-06	7.00E-07	3.48E-07
@fep	4.35E-08	1.27E-07	1.06E-07
@2fep	6.77E-07	1.74E-07	9.57E-08
@3fep	5.84E-08	1.62E-07	9.65E-08

Bilans Session 174			
	Xsat	Ysat	Zat
Angular rate error (rad/s)			
DC	3.92E-09	4.58E-10	2.18E-10
@fep	2.17E-10	3.79E-10	5.01E-11
@2fep	7.50E-09	1.00E-09	4.57E-10
@3fep	1.41E-09	3.38E-10	3.79E-11
Angular acceleration error (rad/s²)			
DC	4.57E-11	5.30E-12	2.55E-12
@fep	7.79E-13	2.21E-12	2.66E-13
@2fep	1.01E-10	9.13E-12	4.70E-12
@3fep	1.97E-11	3.03E-12	6.11E-13

Table 3 : DFACS performance for a slow rotating session MCAs2

6. Conclusion

The on-orbit assessment of Microscope was for the DFACS the confrontation between simulations and reality on a very unusual class of performances. Many technical problems were fixed or passed-by on the star tracker, the propulsion and the instrument. The drag-free performance demonstrated on Microscope is now by far the finest ever achieved on low Earth orbit : $<10^{-12}$ m/s² @Fep, three axis for up to 8 days. The challenge was also on the attitude control: the angular rate stability required $<10^{-9}$ rad/s @Fep was a design driver. The requirement is fulfilled with good margins.

In addition to these performances, Microscope is a great success of architecture with a right association between the key elements: the scientific instrument and the propulsion system. The choice of the CGPS is perfectly adapted to the mission (capacity, performances).

This mission, initiated more than 15 years ago, has been a great personal and collective experience with many moments of doubt. Perhaps Microscope will not find the limits of Einstein's theory, but a new domain of performances is now open: Microscope becomes a reference.

References

- 1) Valerio CIPOLLA, Jean-Bernard DUBOIS, Benjamin POUILLLOUX, Pascal PRIEUR 'Microscope, a microsatellite for Equivalence Principle Measurement in Space', 25th Annual AIAA/USU Conference on Small Satellites, SCC11-I-3
- 2) Pierre-Yves Guidotti & al, MICROSCOPE: 7 months of a very complex commissioning phase toward ultimate performance, COSPAR 2017 (forthcoming)
- 3) Pittet C., Accelero-stellar hybridization for MICROSCOPE drag-free mission , in Proc. ACA 2007, Aerospace Control Application, Toulouse (France), 25-29 juin 2007
- 4) C. Pittet and P. Prieur, 'Structured accelero-stellar estimator for Microscope drag-free mission', in Advances in Aerospace Guidance, Navigation and Control, Springer, CEAS 2015
- 5) Stéphanie Delavault, Pascal Prieur, Thomas Liénart, Alain Robert, Pierre-Yves Guidotti 'MICROSCOPE mission: drag-free and attitude control system expertise activities toward the scientific team', ESA GNC 2017 Salzburg
- 6) Florence Genin and Pascal Prieur 'In-flight assessment of star tracker performances: from Picard, through Prisma, to Microscope' ISSFD 2015
- 7) A. Walker-Deemin, 'Meeting MICROSCOPE's specific attitude-guidance requirements building upon MYRIADE satellite-family's inheritance', 25th International Symposium on Space Flight Dynamics (ISSFD), October 2015
- 8) T. Liénart, K. Pfaab, 'Cold Gas Propulsion System for CNES Microscope spacecraft : presentation of the project and development and verification plan', 49th Joint Propulsion Conference, San Diego 2013.
- 9) G. Noci *et al.*, 'Cold Gas Micro Propulsion for European Science Missions: status on development and achievements under LISA Pathfinder, Microscope and forthcoming Euclid, following the successful delivery and in flight operation of the GAIA Micro Propulsion System' 4th Space Propulsion conference, Cologne 2014 <http://www.propulsion2014.com/>
- 10) J W Conklin *et al.*, 'Precision attitude control of the Gravity Probe B satellite' IOP science 2015
- 11) Le Du M., Maureau J. and Prieur P. (2002). Myriade: an adaptative concept, in Proc. 4thGNC ESA, Frascati.
- 12) David PASCAL & al, Orbit Determination for the MICROSCOPE Mission, Specificities and Performance, ISSFD 2017
- 13) P.S. Jørgensen, J.L. Jørgensen and T. Denver: "μASC: A Miniature Star Tracker", in proceedings of ESA 4S, 20-24 September 2004, La Rochelle, France
- 14) T. Denver, J.L. Jørgensen, R. Michelsen and P.S. Jørgensen: "The MicroASC Star Tracker, Generic Developments and Performance", in proceedings of ESA 4S, 25-29 September 2006, Chia Laguna, Sardinia, Italy